

# Instability of nanometric fluid films on a thermally conductive substrate

N. Dong and L. Kondic

*Department of Mathematical Sciences, New Jersey Institute of Technology, Newark, NJ 07102 USA*

(Dated: December 3, 2024)

We consider thin fluid films placed on thermally conductive substrates and exposed to time-dependent spatially uniform heat source. The evolution of the films is considered within the long-wave framework in the regime such that both fluid/substrate interaction, modeled via disjoining pressure, and Marangoni forces, are relevant. We analyze the problem by the means of linear stability analysis as well as by time-dependent nonlinear simulations. The main finding is that when self-consistent computation of the temperature field is performed, a complex interplay of different instability mechanisms results. This includes either monotonous or oscillatory dynamics of the free surface. In particular, we find that the oscillatory behavior is absent if the film temperature is assumed to be slaved to the current value of the film thickness. The results are discussed within the context of liquid metal films, but are of relevance to dynamics of any thin film involving variable temperature of the free surface, such that the temperature and the film interface itself evolve on comparable time scales.

PACS numbers: 47.55.nb 81.16.Rf, 47.54.Jk 47.20.Dr,

Instabilities of thin fluid films are relevant in a variety of different contexts, with many of these involving temperature variations that lead to modified material properties. In particular, the surface tension of many liquids is sensitive to temperature, resulting in well known Marangoni effect, that has been discussed in excellent review articles [1, 2] and books [3].

Instabilities due to Marangoni effect have been studied extensively, and we will focus here exclusively on the settings that involve deformation of the free surface. The studies are often carried out using the long-wave approach; within this framework, a significant body of work has been established in the recent years, including extensive research on linear and weakly nonlinear instability mechanisms [4–6], as well as discussion of monotone and oscillatory type of Marangoni effect governed instabilities [3, 7–9] (only a subset of relevant works is listed here). While most of the works have focused on the regime where gravitational effects are relevant, there is also an increasing body of work considering the interplay between the instabilities caused by Marangoni effect and by liquid-solid interaction that becomes important for the films on nanoscale, see, e.g., [10–13]. Understanding the influence of Marangoni effect on film stability is simplified in the settings where temperature of the film surface could be related in some simple way to its thickness; however it is not always clear that a simple functional relation can be accurately established, particularly in the setups such that the temperature field and the film thickness evolve on the comparable time scales so that the temperature of the fluid may be history dependent.

One context where thermal effects are relevant involves metal films on nanoscale thickness exposed to laser irradiation. The energy provided by laser pulses melts the films, and, while in the liquid state, these films evolve on a time scale that is often comparable to the pulse duration (tens of nanoseconds). The flow of thermal energy during this short time leads to a complex setup that involves heat flow not only in the metal film but also in the substrate, phase change (both melting and solidification), possible ablation, and chemical effects. Coupling of these effects to fluid dynamical aspects of

the problem is just beginning to be understood [12–16].

This Rapid Communication focuses on fundamental mechanisms involved in the influence of thermal dependence of surface tension for films evolving on thermally conducting substrates. For definitiveness, we use the material parameters appropriate for liquid metals, and consider only the basic aspects of the problem, ignoring the effects of melting/solidification, ablation, or temperature dependence of other material parameters. The substrate is considered to be thermally conductive, but otherwise uniform and of thickness much larger than that of the film. Since the motivation comes from nanoscale films, we do not include gravity, but we do consider substrate/film interaction via disjoining pressure model that allows for natural definition of contact angle. It should be also noted that inclusion of fluid/solid interaction is necessary if one wants to consider film instability on nanoscale. While, as mentioned above, a significant body of work considering the influence of Marangoni forces on thin film stability has been established, we are not aware of any work considering the interplay of Marangoni effect and fluid/solid interaction by fully self-consistent computation of the thin film evolution, and the temperature field, in fully nonlinear regime.

The problem will be considered within the long-wave framework that allows to obtain an insight into the most important aspects of the problems and carry out simulations at modest computational cost. The price to pay is approximate nature of the results, in particular in the context of liquid metal films that are characterized by large contact angles and fast evolution that suggests that inertial effects (not included in the standard version of the long-wave framework considered here) may be relevant. However, despite the fact that all the assumptions involved in deriving long-wave approach are not strictly satisfied, one can obtain reasonably accurate results when using the long-wave approach to explain physical experiments - see, e.g., [17–20], or even when comparing to direct numerical solvers of Navier-Stokes equations [21].

Within the long-wave framework, one reduces the complicated problem of evolving free surface film into a sin-

gle 4th order nonlinear partial differential equation of diffusion type. To model Marangoni effect, it is typically assumed that surface tension,  $\gamma$ , is a linear function of temperature:  $\gamma(T) = \gamma_0 + \gamma_T T$ , where  $\gamma_0 = \gamma(T_0)$ , and  $\gamma_T$  is (for most of the materials) a negative constant. In the present work,  $T$  is defined relative to some reference temperature,  $T_0$  (we will use room temperature), and non-dimensionalized as described below. In non-dimensional form, the evolution equation resulting from conservation of mass of (incompressible) film is as follows

$$\frac{\partial h}{\partial t} + \nabla \cdot (h^3 \nabla^2 h) + K \nabla \cdot [h^3 f'(h) \nabla h] + D \nabla \cdot (h^2 \nabla T) = 0. \quad (1)$$

Here,  $h$  is the film thickness,  $\nabla = (\partial/\partial x, \partial/\partial y)$ , and  $(x, y)$  are the in-plane coordinates. The second term is due to surface tension, and the remaining two terms are due to solid/fluid interaction and Marangoni effect, respectively. The function  $f(h)$ , proportional to disjoining pressure, is assumed to be of the form  $f(h) = (h_*/h)^n - (h_*/h)^m$ , where we use  $(n, m) = (3, 2)$  as motivated by direct comparison to experimental results with Cu films [19]. Next, we define  $t_s = 3\mu l_s/\gamma_0$  as the time scale, where  $l_s$  is a chosen length-scale (we use typical film thickness of 10nm). The non-dimensional parameters are then specified by  $K = \kappa l_s/\gamma_0$ ,  $D = 3\gamma_T/(2\gamma_0)$ , and  $\kappa$  is related to Hamaker's constant,  $A$ , by  $A = 6\pi\kappa h_*^3 l_s^3$ . The reader is referred to Supplementary Materials (SM) [22] for the values of the material parameters used, to [23] for extensive discussion regarding inclusion of disjoining pressure in the long-wave framework, to [15, 17, 19] for the use of the long-wave in the context of modeling liquid metal films, and to [1–3] for the discussion of Marangoni effects in a variety of settings. The numerical solutions of Eq. (1), discussed in what follows, are obtained using the spatial discretization and temporal evolution as described in e.g. [24], with the grid size equal to  $h_*$ ; such discretization is sufficient to ensure accuracy.

So far, the presentation applies to any situation where temperature gradients are present. Let us now focus on the setup of interest here, and that is a film exposed to an external heat source (such as a laser for experiments done with metal films), and is placed on a thermally conductive substrate, such as SiO<sub>2</sub>. To start, consider a spatially uniform film, exposed to an energy source, and in formulating the model describing the temperature of the film, ignore convective effects, and furthermore consider only the heat flow in the  $z$  direction, normal to the plane of the film. Then, the temperature of the film (and of the substrate) can be modeled by diffusion equations (with a source term) for the film and for the substrate, coupled by appropriate boundary conditions

$$\frac{\partial T_i}{\partial t} = K_i \frac{\partial^2 T_i}{\partial z^2} + Q_i, \quad (i = 1, 2), \quad (2)$$

where  $i = 1, 2$  stands for the film and for the substrate phase, respectively. The parameters entering the equation are listed in SM [22], where we also define the temperature scale that is used throughout; here we only note that the source term,  $Q_1$ ,

also includes absorption of heat in the film, and is of the functional form  $Q_1 = CF(t) \exp(-\tilde{\alpha}(z-h))$ , where  $C$  is a constant determined by the intensity of the heat source (laser),  $\alpha$  is the (scaled) coefficient of absorption, and  $z$  is the out-of-plane coordinate. We will assume that the substrate does not absorb heat; this is appropriate for SiO<sub>2</sub> that is transparent to radiation. In fluid modeling that follows, we will also assume that the substrate remains solid. The boundary conditions include no heat transfer at the free surface; in the spirit of the long-wave approach this simplifies to  $\partial T(z)/\partial z|_{z=h} = 0$  even for nonuniform films; at  $z = 0$  we use continuity of temperatures and heat fluxes, therefore ignoring thermal resistance there, and at the bottom of the substrate, we put  $T(-h_s) = 0$  (room temperature). Ignoring heat flow in the in-plane direction can be justified by relatively slow time scale of heat conduction in the substrate (due to low heat conductivity of SiO<sub>2</sub>). Further studies of the importance of the in-plane heat transfer would be however appropriate and should be considered in future work. We note that similar approach (of considering heat transfer in the out-of-plane direction only) has been used in existing studies, see, e.g., [15, 18].

Equations (2) are solved using standard finite difference method, with spatial derivatives discretized using central differences and Crank-Nicolson method implemented for temporal evolution; we use 160 grid points for each of the domains (film, substrate) - this value is sufficient to ensure convergence. Not surprisingly, the numerical solutions show that the temperature of the film is essentially  $z$ -independent, as also discussed in [15]. The outlined thermal problem, for fixed (time-independent)  $h$  and in the limit  $h_s \rightarrow \infty$  also allows for a closed form solution for  $T(h, t)$ ; see [22] for a derivation (we will refer to this solution as the analytical one). Figure 1(a) compares the analytical solution with the numerical one. We see that for large  $h_s$  there is an excellent agreement between the two, as expected. For smaller values of  $h_s$ , the numerically computed temperature saturates due to the boundary condition at  $z = -h_s$ . Figure 1(b) shows  $T$  and  $\partial T/\partial h$  as a function of  $h$  (assumed to be a given constant). The main feature of the solution is that  $T$  is a non-monotonous function of  $h$ ; an intuitive explanation is that for thin films, only limited amount of energy gets absorbed, and the temperature remains low; for very thick films, the temperature remains low due to a large mass of the fluid that needs to be heated; as an outcome, there is a critical thickness at which  $T$  reaches a maximum value.

The next step is to couple the thermal problem with the fluid one and use the  $T$  resulting from Eq. (2) in Eq. (1). For simplicity, we will limit the consideration to two spatial dimensions so that  $h = h(x, t)$  in Eq. (1). An initial insight can be reached by carrying out linear stability analysis (LSA) of a base state of flat film of thickness  $h_0$  perturbed as follows:  $h = h_0(1 + \varepsilon \exp(iqx + \sigma t))$ . Assuming that  $T$  is a linear function of  $h$  (we discuss this further below), with  $\partial T/\partial h = G = \text{const}$ , one finds the dispersion relation  $\sigma(q) = h_0^3 q^2 (-q^2 + P_0)$ , where  $P_0 = K f'(h_0) + D_1/h_0$ , and  $D_1 = (3\gamma_T/(2\gamma)G)$ . Then, for  $P_0 > 0$ , the most unstable wave-

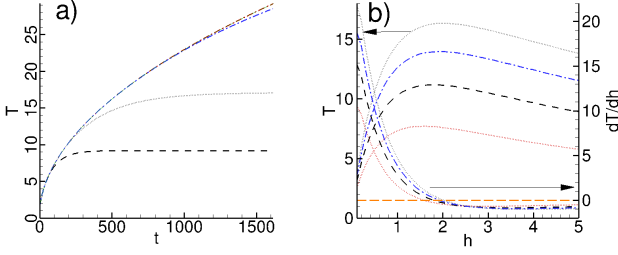


FIG. 1. (Color online) a) Temperature evolution of fixed thickness film under uniform laser pulse computed analytically assuming infinite  $\text{SiO}_2$  thickness  $h_s$  (red dash-dotted), and numerically using  $h_s = 10$  (black long dashed),  $h_s = 20$  (grey dotted),  $h_s = 50$  (blue dash-dotted), and  $h_s = 100$  (green dashed). (Note that the numerical result with  $h_s = 100$  overlaps the analytical one.) b) Temperature and  $\partial T/\partial h$  of the free surface obtained by solving numerically Eq. (2) assuming fixed film thickness,  $h$ . Here,  $t = 100$  (red dotted),  $t = 200$  (black dashed),  $t = 300$  (blue dash-dotted),  $t = 400$  (grey dotted); the arrows indicate the axis related to the set of curves. Orange long dashed line indicates  $\partial T/\partial h = 0$ . We use  $F(T) = \text{const}$ . In this and all the following figures the material and laser properties are from Table 1 in SM [22] if not specified differently.

length,  $\lambda_m$ , and the corresponding growth rate,  $\sigma_m$ , are

$$\lambda_m = \frac{2\pi}{\sqrt{P_0/2}}, \quad \sigma_m = \frac{h_0^3 P_0^2}{4}, \quad (3)$$

Considering now the films of dimensionless thickness  $h_0 \approx 1$ , we see from Fig. 1 that  $G > 0$  and therefore Marangoni effect is stabilizing: the LSA suggests exponential decay of any perturbation for such films since  $P_0 < 0$ . For thicker films, LSA predicts instability; however note that for such films  $|G|$  is rather small (for the present choice of parameters), and destabilizing effect of disjoining pressure is very weak, so that evolution is expected to proceed with small growth rate, suggesting that instability could occur only on very long time scales.

The analytical solution, plotted in Fig. 1 and discussed in SM [22], as well as the numerical solutions shown in Fig. 1 assume that the film itself does not involve. However, since thermal and fluid problem are coupled, and furthermore since they evolve on comparable time scales (as it will become obvious from the following results, or based on simple dimensional arguments for the time scale governing the heat flow compared to the inverse of the growth rate for film instability), it is not clear that this assumption is appropriate, and it is also not obvious what is its influence on the results. To answer these questions, we will next consider fully coupled problem, where we solve numerically Eq. (1), while self-consistently computing the temperature by solving the system of diffusion Eqs. (2). We will first consider uniform source term, and then a Gaussian one. The initial condition is a film perturbed by a single cosine-like perturbation of the wavelength corresponding to  $\lambda_m$  obtained from the LSA with Marangoni effect excluded. The initial temperature (at  $t = 0$ ) of the film and the substrate is taken to be the room temperature, so  $T(t = 0) = 0$ .

Figure 2 shows few snapshots of  $h$ ,  $T$ , and  $\partial T/\partial h$ . Initially, (a)  $h$  is perturbed, and  $T$  is constant. The perturbation in  $h$  grows (b) due to destabilizing disjoining pressure, and leads to a perturbation in  $T$ . This perturbation stabilizes the film (the fluid flows from hot to cold), leading to essentially flat  $h$ , but  $T$  and  $\partial T/\partial h$  are delayed and are not uniform (c). This nonuniform temperature induces further evolution of the film profile and ‘inverted’ perturbation (d), that is again stabilized by Marangoni flow. This process continues, leading to damped oscillatory evolution of the film.

Figure 3 shows the film thickness at the middle of the domain,  $h_m = h(x_m = \lambda_m/2)$  as a function of time for few different approaches used to compute the film temperature: (i) the self-consistent time-dependent solution of Eq. (2) coupled with Eq. (1) (the same approach used to obtain the results shown in Fig. 2); (ii) the analytical solution of Eq. (2) assuming fixed film thickness, and (iii) linear temperature assuming fixed  $G = 3.0$  (see Fig. 1b)). The evolution in the absence of Marangoni effects is shown as well - here, the film destabilizes on the time scale expected from the LSA. For self-consistent temperature computations,  $h_m$  shows oscillatory behavior, in contrast to the other considered approaches for temperature computations, or when Marangoni effect is not included. Note that the numerical solution uses  $h_s = 100$ ; for such  $h_s$ , there is an excellent agreement between the numerical and analytical temperature solutions for fixed film thickness, see Fig. 1a). Therefore, the difference between the solutions is not due to analytical solution not being accurate, but due to the fact that it ignores evolution of the film itself.

Our finding so far is that Marangoni effect, when included self-consistently into Eq. (1), changes dramatically the behavior of the film, leading to stabilization for the present choice of parameters. The effect is particularly dramatic for thin films, that are strongly unstable due to destabilizing disjoining pressure, if Marangoni effect is excluded. The obvious question is whether these results are general, in particular in the light of experimental findings that find instability, see, e.g., [13, 19]. To start answering this question, we consider the influence of two parameters: time dependence of the source term, and its total energy. Further more detailed study of the influence of other parameters will be given elsewhere [25].

Figure 4 shows  $h_m$  obtained by assuming Gaussian profile (function  $F(t)$ ) of the source of different widths (see SM [22] for more details), keeping the total energy the same as for the uniform profile considered so far. From Fig. 4, we observe that as the energy distribution of the source becomes more narrow, the oscillatory behavior of  $h_m$  becomes stronger; however we always find that the final outcome is consistent with the one obtained for a uniform source - stable film.

Figure 5 shows the results obtained for the same setup as in Fig. 4 but with decreased energy of the pulse. Now, the evolution is unstable: while Marangoni effect is strong enough to suppress initial instability growth (decrease of  $h_m$ ), it is insufficient to stabilize the rebound:  $h_m$  increases monotonously for later times, with the final outcome (for longer times than shown in Fig. 5) of formation of a drop centered at  $x_m$ . Other

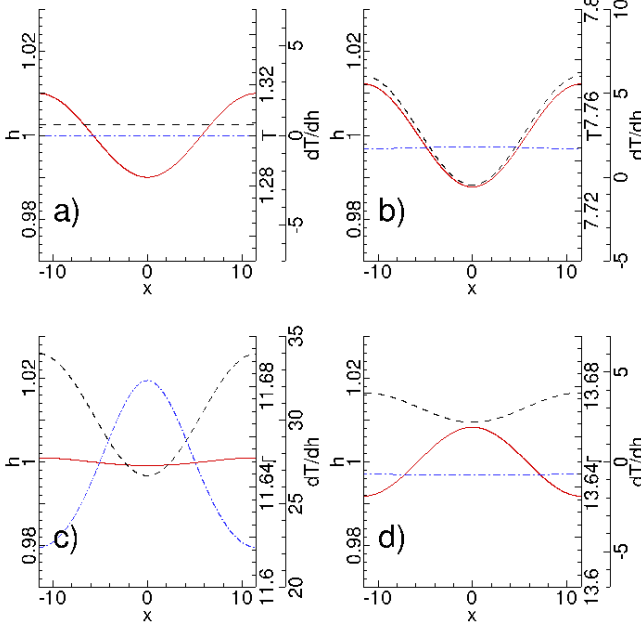


FIG. 2. (Color online) Evolution of the film thickness,  $h$  (red solid), temperature,  $T$  (black dashed), and temperature gradient,  $\partial T/\partial h$  (blue dash dotted) as a result of self-consistent time-dependent computations of the film thickness and temperature. The domain size is  $\lambda_m$  defined by Eq. (3) without Marangoni effect ( $D_1 = 0$ ). The times shown are:  $t = 0$  (a),  $t = 113$  (b),  $t = 258$  (c),  $t = 355$  (d).

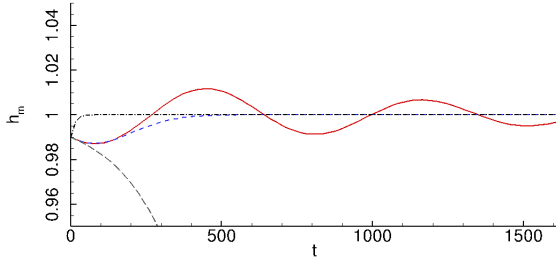


FIG. 3. The film thickness,  $h_m$ , at  $x_m = \lambda_m/2$  using different approaches to compute the temperature: self consistent time-dependent temperature computation (red solid), the analytical solution of Eq. (2) assuming fixed film thickness (blue dashed), and assuming fixed  $G = 3.0$  (black dash dotted). The evolution computed by ignoring Marangoni effect all together is shown as well (grey long dashed).

outcomes are possible: e.g., for the total energy at some intermediate level between the ones used in Figs. 4 and 5, one can find drops centered at the domain boundaries (results now shown for brevity).

The main conclusion of this work is that careful consideration of nonlinear effects is required to properly account for the influence of Marangoni forces on the film evolution: in particular, the assumption that the film temperature is slaved to its thickness leads to different results from the ones obtained by self-consistent computations. The sensitivity of the outcome as the parameters entering the problem (such as time

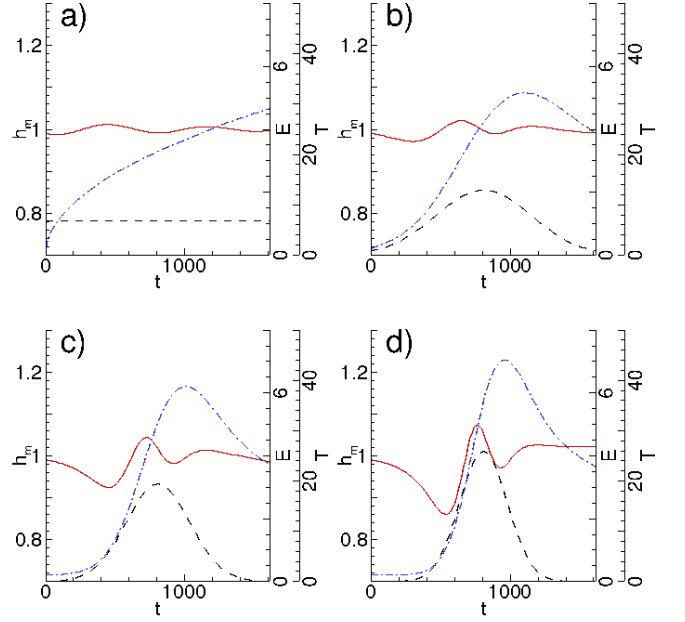


FIG. 4. The film thickness,  $h_m$  (red solid), numerically computed film temperature at  $x_m$  (blue dash dotted), and the applied energy distribution (black dashed). The total energy applied during considered time window is kept constant.

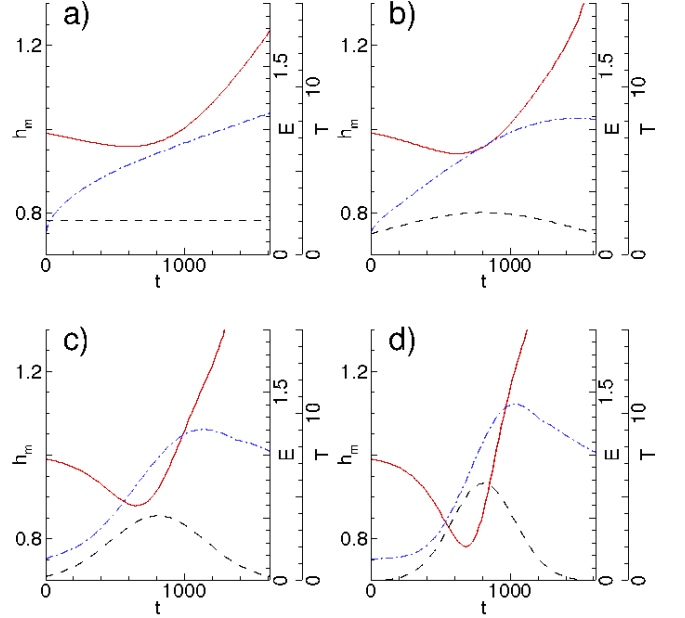


FIG. 5. The film thickness,  $h_m$  (red solid), numerically computed film temperature at  $x_m$  (blue dash dotted), and the applied energy distribution (black dashed). The total energy applied is kept constant at the value equal to  $1/4$  of the one used in Fig. 4. Note different scales for  $T$  and  $E$  compared to Fig. 4.

dependence of the heat source or its total energy) are changed suggests that more general insight could be reached by carry-

ing out further study using more elaborate linear and weakly-nonlinear analyses of the evolution. We hope that our results will inspire further research in this direction.

We note that in the present work we consider rather simple setup limited to two spatial dimensions only, and also we focus on a single perturbation of a fixed wavelength evolving in the computational domain of the size of the wavelength. However, already in such a setup we find rather complex coupling of thermal and fluid aspects of the problem. These results show that Marangoni effect may influence significantly the stability of the films in the context relevant to applications; they also suggest that Marangoni effect may modify both the emerging length-scales, and the time-scales on which they appear. To further explore the influence of Marangoni effect in more general settings, one would need to consider three dimensional setup in larger computational domains. Furthermore, in the direction of applying the results to metal films irradiated by laser pulses, solidification/melting as well as modification of other physical parameters (such as viscosity) due to temperature variation should be considered. These directions will be explored in our future works.

*Acknowledgements* The authors thank Shahriar Afkhami, Jason Fowlkes, Kyle Mahady, Philip Rack, and Ivana Seric for many insightful discussions. This work was partially supported by the NSF Grant No. CBET-1235710.

## APPENDIX

### Parameters

Table I provides the parameters and scales used in the main text. The film parameters (subscript ‘m’) assume Cu film, and the substrate parameters (subscript ‘s’) assume SiO<sub>2</sub>.

### Formulation of the heat diffusion problem

The dimensional heat diffusion equation with the time dependent source term, considered in the main text, is as follows

$$(\rho C_{eff})_m \frac{\partial T}{\partial t} = k_m \frac{\partial^2 T}{\partial z^2} + S^* F(t) \alpha_m e^{-\alpha_m(z-h)}. \quad (4)$$

Here we take the film surface to be at  $z = h$ , and the film-substrate interface is at  $z = 0$ . In the substrate layer, the heat absorption is ignored, leading to

$$(\rho C_{eff})_s \frac{\partial T}{\partial t} = k_s \frac{\partial^2 T}{\partial z^2}. \quad (5)$$

The scales and parameters are given in Table I. For uniform pulse we have

$$S^* = [1 - R(h)] \frac{E_0}{t_p}; \quad F(t) = 1.$$

| Parameter  | Value                  | Unit              |
|--|------------------------|-------------------|
| viscosity ( $\mu$ )                                | $4.3 \times 10^{-3}$   | m <sup>2</sup> /s |
| surface tension ( $\gamma$ )                       | 1.303                  | J/m <sup>2</sup>  |
| length scale ( $l_s$ )                             | $1.0 \times 10^{-8}$   | m                 |
| time scale ( $t_s = 3l_s\mu/\gamma$ )              | $9.21 \times 10^{-11}$ | s                 |
| film density ( $\rho_m$ )                          | $8.0 \times 10^3$      | kg/m <sup>3</sup> |
| SiO <sub>2</sub> density ( $\rho_{SiO_2}$ )        | $2.2 \times 10^3$      | kg/m <sup>3</sup> |
| film heat capacity ( $C_{eff,m}$ )                 | $4.95 \times 10^2$     | J/kg/K            |
| SiO <sub>2</sub> heat capacity ( $C_{eff,SiO_2}$ ) | $9.37 \times 10^2$     | J/kg/K            |
| film heat conductivity ( $k_m$ )                   | $3.40 \times 10^2$     | W/m/K             |
| film absorption length ( $\alpha_m^{-1}$ )         | $11.09 \times 10^{-9}$ | m                 |
| SiO <sub>2</sub> heat conductivity ( $k_{SiO_2}$ ) | $1.4 \times 10^0$      | W/m/K             |
| surface tension dep of T ( $\gamma_T$ )            | $-2.3 \times 10^{-4}$  | J/m <sup>2</sup>  |
| Avogadro’s constant ( $A$ )                        | $1.83 \times 10^{-18}$ | J                 |
| reflective coefficient ( $r_0$ )                   | 0.3655                 | 1                 |
| film reflective length ( $\alpha_r^{-1}$ )         | $12.0 \times 10^{-9}$  | m                 |
| laser energy density ( $E_0$ )                     | $8.80 \times 10^3$     | J/m <sup>2</sup>  |
| time duration of observation ( $t_{total}$ )       | 160                    | ns                |
| Gaussian pulse peak time ( $t_p$ )                 | 80                     | ns                |
| equilibrium film thickness ( $h_*$ )               | $1.0 \times 10^{-10}$  | m                 |
| film thickness ( $h_0$ )                           | $1.0 \times 10^{-8}$   | m                 |
| SiO <sub>2</sub> thickness ( $h_{SiO_2}$ )         | $1.0 \times 10^{-6}$   | m                 |
| room temperature ( $T_{room}$ )                    | 300                    | K                 |

TABLE I. The parameters used in the main text.

where  $R(h)$  is the overall material reflectivity.

$$R(h) = r_0(1 - e^{-\alpha_r h})$$

For Gaussian pulse,

$$S^* = [1 - R(h)] \frac{E_0 \zeta}{\sqrt{2\pi\sigma}}; \quad F(t) = \exp(-(t - t_p)^2 / \sigma^2),$$

Here,  $\zeta$  is a renormalization factor used to ensure that during the considered observation time,  $t_{total}$ , the Gaussian and the uniform pulse lead to the same total applied energy.

Equation (2) from the main body of the text is obtained by using the length and time scale as defined there, and the temperature scale  $T_s = t_s E_0 \alpha_m / (\rho C_{eff})_m t_p$ :

$$K_1 = \frac{k_m t_s}{(\rho C_{eff})_m l_s^2}$$

$$Q_1 = \frac{t_s S^* F(t) \alpha_m e^{-\alpha_m(z-h)}}{(\rho C_{eff})_m T_s}$$

$$K_2 = \frac{k_s t_s}{(\rho C_{eff})_s l_s^2}; \quad Q_2 = 0$$

### Outline of the derivation of the analytical solution to the heat diffusion problem

Here, we give a brief overview of the derivation of the analytical solution of Eqs. (4-5), assuming that the film thickness

is constant (or, equivalently, that the temperature is slaved to the current value of the film thickness), assuming also that the substrate layer is infinitely thick. This formulation was discussed in more details in [15], and also used for the purpose of estimating liquid lifetime of metal film in [16, 18, 20]. Let

$$S = \frac{S^*[1 - e^{-\alpha_m h}]}{(\rho C_{eff})_m h}; \quad K = \frac{\sqrt{(\rho C_{eff} k)_s}}{(\rho C_{eff})_m h},$$

and

$$q_s(t) = -k_m(\partial T / \partial z)_m = -k_s(\partial T / \partial z)_s.$$

Here  $q_s(t)$  represents the heat flux through the film-substrate interface. Since the film layer is thin and the heat conduction high, the time scale for heat conduction in the  $z$  direction is short,  $\approx 10^{-2}$  ns using the parameters as given in Table I. There, the approximation that  $T \neq f(z)$  is expected to be highly accurate. Integrating Eq. (4) from  $z = h$  to  $z = 0$  and taking the average, we find

$$T(t) = T_0 + \int_0^t \left( S f(\tau) - \frac{q_s(\tau)}{(\rho C_{eff})_m h} \right) d\tau \quad (6)$$

Solving the heat equation in the substrate of semi-infinite thickness gives

$$T_s(t, z) = T_0 + \frac{\sqrt{\alpha_s}}{k_s \sqrt{\pi}} \int_0^t q_s(\tau) (t - \tau)^{\frac{1}{2}} \exp\left(\frac{-z^2}{4\alpha_s(t - \tau)}\right) d\tau$$

Using  $T(t) = T_s(t, 0)$  we have

$$S \int_0^t f(\tau) d\tau = \int_0^t \frac{q_s(\tau) d\tau}{(\rho C_{eff})_m h} + \frac{\sqrt{\alpha_s}}{k_s \sqrt{\pi}} \int_0^t \frac{q_s(\tau)}{\sqrt{t - \tau}} d\tau$$

Using Laplace transform, we can solve for  $q_s(t)$ , and substituting the result into Eq. (6), we obtain the solution for the film temperature

$$T(t) = T_0 + S \int_0^t e^{K^2 u} \operatorname{erfc}(K \sqrt{u}) du. \quad (7)$$

This  $T(t)$  is shown in the main body of the paper as the analytical solution. Note that its derivation assumes that  $h$  remains constant in time.

- [2] R. Craster and O. Matar, *Rev. Mod. Phys.* **81**, 1131 (2009).
- [3] P. Colinnet, J. Legros, and M. Velarde, *Nonlinear dynamics of surface-tension-driven instabilities* (Wiley-VCH, Berlin, 2001).
- [4] A. Podolny, A. Oron, and A. A. Nepomnyashchy, *Phys. Fluids* **17**, 104104 (2005).
- [5] M. Morozov, A. Oron, and A. A. Nepomnyashchy, *Phys. Fluids* **27**, 082107 (2015).
- [6] A. Nepomnyashchy and I. Simanovskii, *J. Fluid Mech.* **771**, 159 (2015).
- [7] S. Shklyaev, M. Khenner, and A. A. Alabuzhev, *Phys. Rev. E* **82**, 025302 (2010).
- [8] S. Shklyaev, A. A. Alabuzhev, and M. Khenner, *Phys. Rev. E* **85**, 016328 (2012).
- [9] A. E. Samoilova and N. I. Lobov, *Phys. Fluids* **26**, 064101 (2014).
- [10] M. R. E. Warner, R. V. Craster, and O. K. Matar, *Phys. Fluids* **14**, 1642 (2002).
- [11] A. Atena and M. Khenner, *Phys. Rev. B* **80**, 075402 (2009).
- [12] M. Khenner, S. Yadavali, and R. Kalyanaraman, *Phys. Fluids* **23**, 122105 (2011).
- [13] J. Trice, D. Thomas, C. Favazza, R. Sureshkumar, and R. Kalyanaraman, *Phys. Rev. Lett.* **101**, 017802 (2008).
- [14] V. Ajaev and D. Willis, *Phys. Fluids* **15**, 3144 (2003).
- [15] J. Trice, D. Thomas, C. Favazza, R. Sureshkumar, and R. Kalyanaraman, *Phys. Rev. B* **75**, 235439 (2007).
- [16] C. A. Hartnett, K. Mahady, J. D. Fowlkes, S. Afkhami, L. Kondic, and P. D. Rack, *Langmuir* **31**, 13609 (2015).
- [17] L. Kondic, J. Diez, P. D. Rack, Y. Guan, and J. Fowlkes, *Phys. Rev. E* **79**, 026302 (2009).
- [18] J. D. Fowlkes, L. Kondic, J. Diez, and P. Rack, *Nano Letters* **11**, 2478 (2011).
- [19] A. Gonzalez, J. Diez, Y. Wu, J. Fowlkes, P. Rack, and L. Kondic, *Langmuir* **13**, 9378 (2013).
- [20] J. D. Fowlkes, N. A. Roberts, Y. Wu, J. A. Diez, A. G. González, C. Hartnett, K. Mahady, S. Afkhami, L. Kondic, and P. Rack, *Nano Letters* **14**, 774 (2014).
- [21] K. Mahady, S. Afkhami, J. Diez, and L. Kondic, *Phys. Fluids* **25**, 112103 (2013).
- [22] “See supplementary material at [URL will be inserted by AIP].”
- [23] J. Diez and L. Kondic, *Phys. Fluids* **19**, 072107 (2007).
- [24] J. Diez and L. Kondic, *J. Comput. Phys.* **183**, 274 (2002).
- [25] N. Dong and L. Kondic, (2016), in preparation.

---

[1] A. Oron, S. H. Davis, and S. G. Bankoff, *Rev. Mod. Phys.* **69**, 931 (1997).